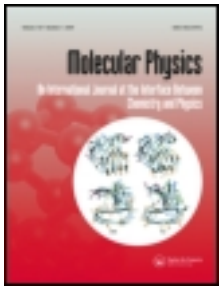

Molecular Physics: An International Journal at the Interface Between Chemistry and Physics
Publication details, including instructions for authors and subscription information:
http://www.tandfonline.com/loi/tmph20

Variation of reactivity of aziridinium ion during alkylation

Sourab Sinha [a] & Pradip Kr. Bhattacharyya [a]
[a] Department of Chemistry , Arya Vidyapeeth College , Guwahati , Assam , India
Accepted author version posted online: 10 Apr 2013.Published online: 07 May 2013.

To cite this article: Sourab Sinha & Pradip Kr. Bhattacharyya (2013): Variation of reactivity of aziridinium ion during alkylation, Molecular Physics: An International Journal at the Interface Between Chemistry and Physics, DOI:10.1080/00268976.2013.794312

To link to this article: http://dx.doi.org/10.1080/00268976.2013.794312

Molecular Physics, 2013
http://dx.doi.org/10.1080/00268976.2013.794312

Variation of reactivity of aziridinium ion during alkylation

Sourab Sinha and Pradip Kr. Bhattacharyya*

Department of Chemistry, Arya Vidyapeeth College, Guwahati, Assam, India

(*Received 26 January 2013; final version received 28 March 2013*)

Reactivity/stability of the tricyclic aziridinium ion intermediate of the mustine drug molecule varies with the ∠NCC bond angle of the tricyclic ring during alkylation of guanine. A sharp variation in reactivity of the aziridinium ion intermediate is observed along the intrinsic reaction coordinate. Further, shifting of the lowest unoccupied molecular orbital towards the carbon centre that interacts with guanine is also observed. Thermochemical analysis shows that the alkylation reaction is exothermic and presence of polar solvent effect activation energy.

Keywords: aziridinium ion; DNA alkylation; DFRT; reactivity descriptors; structural variation

1. Introduction

Mustine, the earliest and perhaps the most extensively studied and clinically employed DNA inter-strand cross-linking agent is being used in cancer chemotherapy for more than 50 years [1–4]. Mode of action of this drug molecule is well understood, and it has been confirmed that its cytotoxicity is allied with its alkylating ability by means of reaction with biomolecules preferentially to nucleophilic centres in DNA bases [5,6]. Mustine forms a very reactive aziridinium (Az^+) ion intermediate and preferential alkylation at the endocyclic nitrogen and exocyclic oxygen atoms of DNA bases is the suggested mechanism [7,8]. Earlier works confirmed that out of different nucleophilic sites in DNA bases, N7 position of guanine is the most nucleophilic and was shown to be a highly preferred site over others for alkylation [9–16]. Recently, Mann made an explicit study on formation of Az^+ ion of nitrogen mustards using *ab initio* dynamics [17]. During alkylation, each of the chloroethyl side chains of the nitrogen mustards (a) spontaneously cyclises to form Az^+ ion (b) that finally binds to N7 of guanine in DNA, resulting a mono-adduct (c) [18–21] (Figure 1).

During alkylation at N7 of guanine, the Az^+ ion accepts electron density from N7 centre, and therefore, position as well as stability of the LUMO (lowest unoccupied molecular orbital) of the Az^+ ion becomes important [22–24]. Our earlier works suggest that reactivity of the Az^+ ion intermediate depends on its structure as well as on the direction of external electric field [25]. It is important to note that in its stable conformation, ∠N3C2C1 ≈ 60°, the LUMO is mostly localised on the chloroethyl side chain (Figure 1(d)), which rule out the interaction between C1 of Az^+ ion and N7 of guanine. Thus, shape of LUMO as well as reactivity of the Az^+ ion happens to be important during the alkylation process.

It is well known that the structure of an intermediate species plays an important role in its chemical as well as biochemical reactions, and during the course of a reaction, intermediates undergo some structural changes [26]. Importantly, reactivity of a chemical species depends on its structure. Dependence of reactivity of a chemical species on its structure was well demonstrated by Pal *et al*. [27] and variation of reactivity descriptors along intrinsic reaction coordinate (IRC) of a reaction was illustrated by Chattaraj *et al*. [28]. During alkylation reaction, as the Az^+ ion approaches DNA (towards guanine base), its structure is expected to vary. Therefore, we examined structural variations and shape of LUMO during alkylation and tried to follow how reactivity of the Az^+ ion varies as it approaches guanine moiety (for check of simplicity glycosidic linkage is replaced by a methyl group). To observe the structural variations on the Az^+ counterpart along the IRC, we performed constrained optimisation on the mustine-guanine mono-adduct for different values of C1–N7 bond length ('*d*', the IRC). Thereafter, guanine moiety was removed and local reactivity descriptors and LUMO shapes of the Az^+ ion intermediate were analysed. The transition state (TS) of the alkylation reaction was obtained by QST2 method [29].

Global parameters (global electrophilicity, ω, and global hardness, η) and local parameters (nucleophilic Fukui function, f^+, and local electrophilicity, ω^+) from density functional reactivity theory (DFRT) were used to characterise variations in reactivity pattern along the IRC. These descriptors are defined within the framework of

*Corresponding author. Email: prdpbhatta@yahoo.com

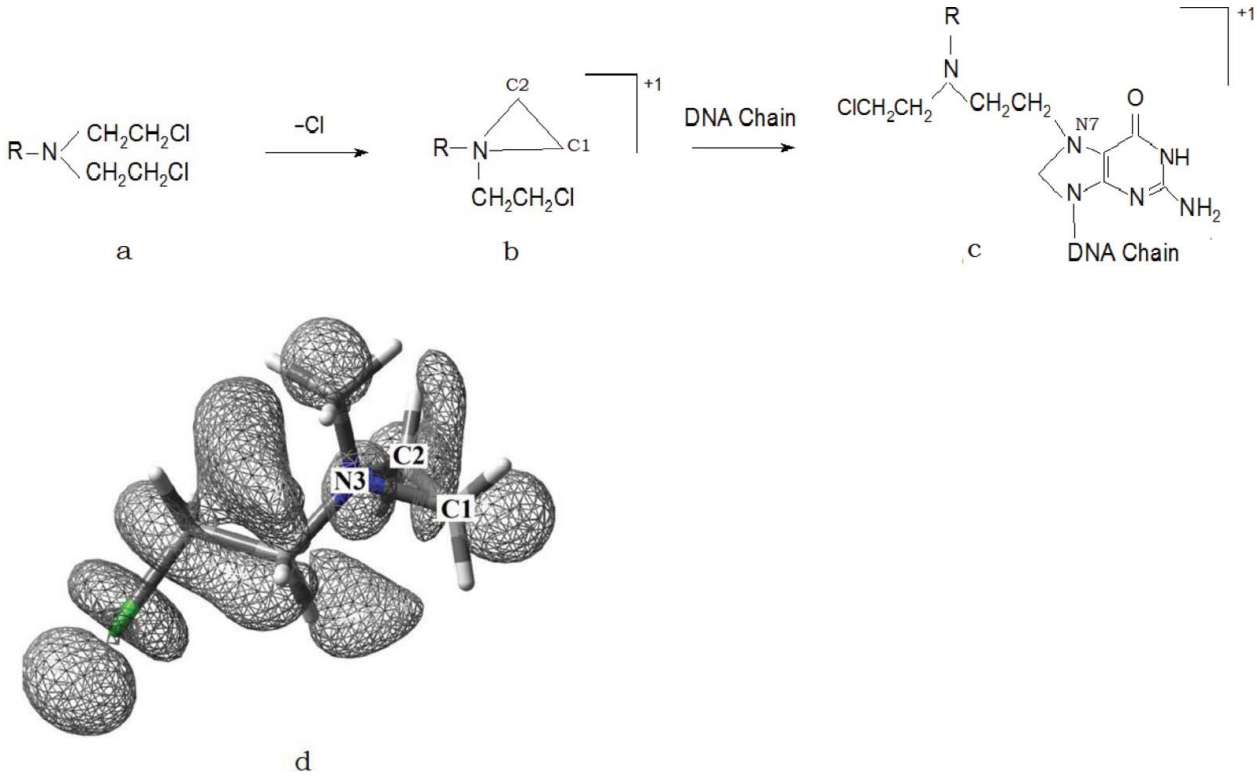

Figure 1. Mechanism of alkylation of DNA by bisalkylating nitrogen mustard.

density functional theory and have been tested and studied in the literature by several research groups and are found to be very useful in rationalising the reactivity patterns of the molecular systems [30–32]. Theoretical basis for these descriptors and their applications in various molecular systems have recently been reviewed well [33,34]. Apart from that we performed thermochemical study and obtained the rate constant of formation of mono-adduct using transition state theory (TST).

2. Theoretical details of reactivity descriptors

Pearson and Parr were the first to provide the definition of global hardness (η) of a chemical species in terms of chemical potential (μ) [35,36]. According to them

$$\eta = \frac{1}{2}\left(\frac{\partial^2 E}{\partial N^2}\right)_{v(\vec{r})} = \frac{1}{2}\left(\frac{\partial \mu}{\partial N}\right)_{v(\vec{r})}, \tag{1}$$

where E is the energy of the system and N is the number of electrons of an electronic system at constant external potential, $v(\vec{r})$. Use of finite difference approximation gives the expressions for μ and η as $\mu = \frac{-IP-EA}{2}$ and $\eta = \frac{IP-EA}{2}$. Koopmans' theorem [37] defines the IP and EA in terms of the energies of highest occupied molecular orbital ($\varepsilon_{\mathrm{HOMO}}$) and lowest unoccupied molecular orbital ($\varepsilon_{\mathrm{LUMO}}$) as IP $= -\varepsilon_{\mathrm{HOMO}}$ and EA $= -\varepsilon_{\mathrm{LUMO}}$. This leads to the expressions for μ and η as

$$\eta = \frac{\varepsilon_{\mathrm{LUMO}} - \varepsilon_{\mathrm{HOMO}}}{2} \tag{2}$$

and

$$\mu = \frac{\varepsilon_{\mathrm{LUMO}} + \varepsilon_{\mathrm{HOMO}}}{2}. \tag{3}$$

Parr and co-workers proposed global electrophilicity (ω) as a measure of electrophilicity of a ligand as [38]

$$\omega = \frac{\mu^2}{2\eta}, \tag{4}$$

The Fukui function is the most important local reactivity index to observe reactivity at particular atomic site, defined as [39]

$$f(r) = \left(\frac{\partial \mu}{\partial v(r)}\right)_N = \left(\frac{\partial \rho(r)}{\partial N}\right)_{v(\vec{r})}. \tag{5}$$

Mendez and Gazquez [40] and Yang and Mortier [41] introduced the procedure to obtain $f(r)$, and using finite difference approximation, the condensed Fukui function

for a nucleophilic attack on the system becomes

$$f_x^+ = [\rho_x(N_0 + 1) - \rho_x(N_0)], \tag{6}$$

where $\rho_x(N_0)$ and $\rho_x(N_0 + 1)$ are electronic population on atom x of the molecule with N_0 and $N_0 + 1$ electron systems, respectively. Roy *et al*. showed that sign of Fukui function is sensitive to the population analysis, and Hirshfeld population is proved to be a better one over Mullikan population analysis [42,43]. The local counterpart of these parameters effectively describes the reactivity at a particular centre. Local electrophilicity is defined as

$$\omega_x^+ = \omega f_x^+. \tag{7}$$

Similar to Fukui functions, using finite difference approximation, Roy *et al*. have proposed local softness at a particular centre as [44]

$$s_x^+ = [\rho_x(N_0 + 1) - \rho_x(N_0)]S \text{ for nucleophilic attack,} \tag{8a}$$

$$s_x^- = [\rho_x N_0 - \rho_x(N_0 - 1)]S \text{ for electrophilic attack} \tag{8b}$$

and

$$s_x^0 = \frac{1}{2}[\rho_x(N_0 + 1) - \rho_x(N_0 - 1)]S \text{ for radical attack.} \tag{8c}$$

They have also proposed 'relative electrophilicity' and 'relative nucleophilicity' as s_x^+/s_x^- and s_x^-/s_x^+, respectively. Local electrophilic or nucleophilic nature of a site is well described by these two descriptors, and their validity was tested on a number of occasions [45–47].

3. Computational details

Structure of the species were optimised using B3LYP/6-31 + G(d) level of theory in gas phase. Real frequency of the systems confirmed that they are at minima. Initially, we performed complete optimisation on the mono-adduct, and thereafter, constraint optimisations were performed on different configurations of the adduct using same level of theory to follow the IRC pathway. Global and local reactivity parameters and LUMO of the Az^+ ion were obtained by disconnecting the guanine moiety and performing single point calculations. Genuineness of the TS geometries were confirmed by an imaginary frequency of the vibrational mode corresponding to the C1—N7 bond. The global reactivity descriptors chemical potential, global hardness and global electrophilicity were calculated from Equations (2)–(4), and the local descriptors were obtained by using Equations (6)–(8). Hirshfeld population analysis was adopted to calculate Fukui functions, local electrophilicity, relative electrophilicity and relative nucleophilicity. All calculations were performed using Gaussian 09 [48]. Reactivity indices were also computed in solvent phase using PCM (Polarisable Continuum Model) and water as solvent [49,50]. Additionally, to check the consistency of our results, single point calculations with a triple zeta basis set 6-311 + + G(d,p) were performed using the same functional.

4. Results and discussion

4.1. Variation of structure of the aziridinium ion along the IRC

Configurations of the Az^+ ion along the IRC obtained at B3LYP/6-31 + G(d) level of theory are summarised in Figure 2. The alkylation reaction is observed to pass through a TS as suggested by earlier works [51,52]. It is interesting to see that for $d > 2.30$ Å, the Az^+ ion retains its typical tricyclic structural parameters with ∠N3C2C1≈60.0° and both N–C (ring carbon) distances = 1.59 Å (Figure 2(a)). As 'd' gets shorter, interaction between the two species takes place and at $d \approx 2.30$ Å, the ring starts to open up. The TS is located at $d = 2.12$ Å and ∠C1C2N3 = 79.9° (Figure 2(b)); exceptional variations in structural parameters are observed around the TS (Figure 2(d)). Beyond the TS, steady variations in these parameters are observed, and finally, it forms the mono-adduct with ∠C1C2N3 = 109.4° and C1—N7 = 1.48 Å (Figure 2(c)). Figure 2(d) summarises the variation of the structural parameters where we observed a sharp variation around the TS. Structure of an intermediate as well as shape of its frontier molecular orbitals (FMOs) around the TS is very crucial, as it directs the reaction either way on the potential energy surface. In earlier works, though mono-adduct formation reaction were studied, this variations were not observed [15,16]. Similar observation was made with triple zeta basis set.

4.2. Variation of shape and energy of LUMO of the drug intermediate

To observe variation of shape and energy of the LUMO, we performed single point calculations on the Az^+ ion obtained from constraint optimised adduct using B3LYP/6-31 + G(d) levels of theory (Figure 3). Our study shows that presence of the guanine moiety at a distance exerts no effect on ε_{LUMO}; at $d = 2.6$ Å, ε_{LUMO} is quite high (= −0.1599 a.u.). As the reaction progresses, Az^+ ion approaches towards guanine, and as a result of interaction between the two, a sharp drop in ε_{LUMO} is observed. At the TS, $\varepsilon_{LUMO} = -0.2725$ a.u., and at $d = 2.0$ Å, $\varepsilon_{LUMO} = -0.3374$ a.u. (Figure 3). This lowering in ε_{LUMO} makes acceptance of electron density by the Az^+ ion more feasible and this in turn facilitates alkylation.

As mentioned earlier, the LUMO of the Az^+ ion is associated mostly at the chloroethyl side chain when the guanine is far apart from the Az^+ ion (e.g. at $d = 2.6$ Å)

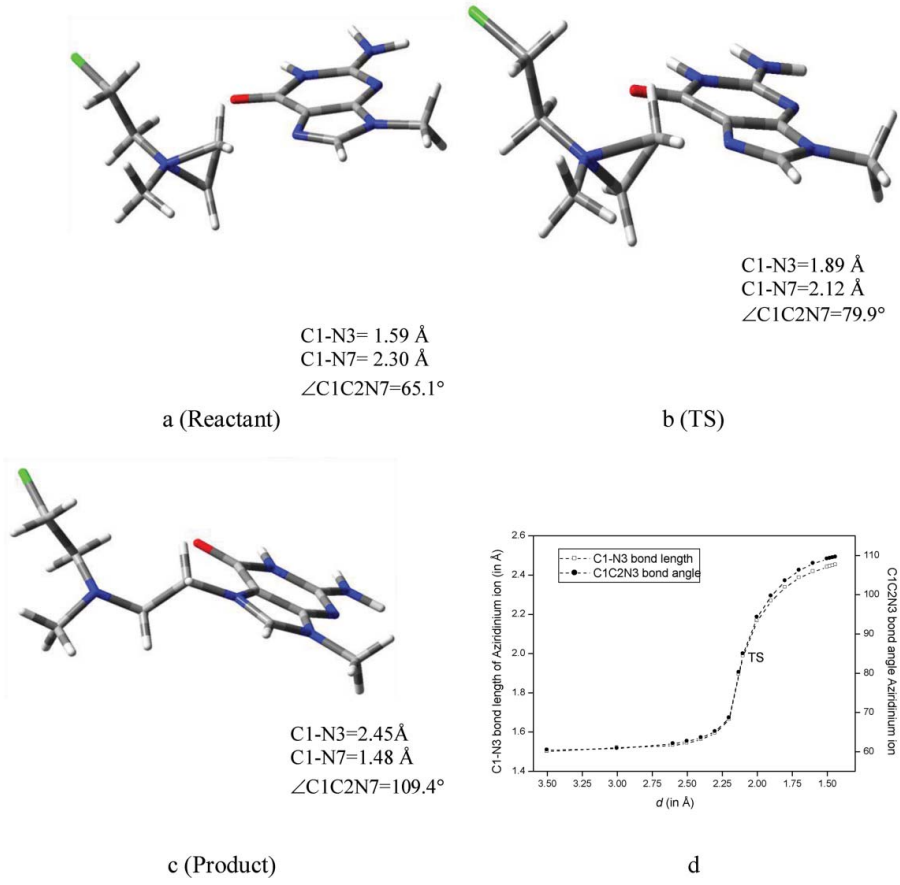

Figure 2. Variation of structure of the Az^+ ion during mono-adduct formation (at B3LYP/6-31 + G(d) level of theory).

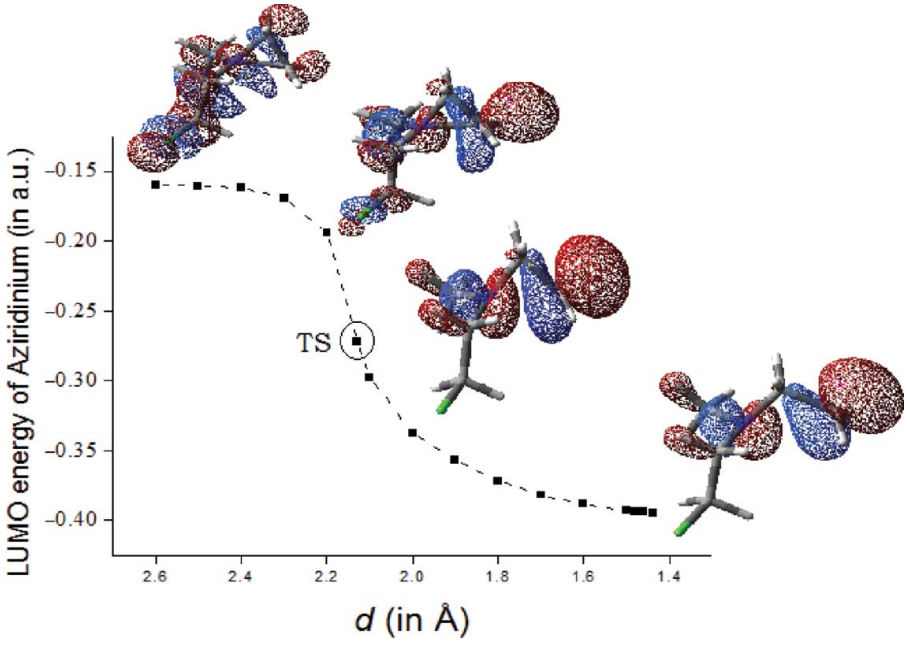

Figure 3. Variation of shape of LUMO of Az^+ ion along the IRC.

(Figure 3). During the course of the reaction, we observe a significant variation in the shape of the LUMO. Around $d = 2.2$ Å, we detect shifting of the LUMO towards the C1 centre of the Az^+ ion and the shifting almost completes before attaining the TS. Shifting of the LUMO of the Az^+ ion is very much essential for the alkylation process to take place. Thus, as Az^+ ion approaches guanine moiety, shifting of the LUMO towards C1 centre facilitates the alkylation process. Results obtained using triple zeta basis set is consistent with the B3LYP/6-31 + G(d) results (Supplementary Material 1).

4.3. Variation of the local and global reactivity descriptors of the aziridinium ion

During the alkylation process, nucleophilic attack takes place on the carbon centres of the Az^+ ion, and hence, it is essential to observe how local reactivity of the carbon centres varies along the IRC. As Az^+ ion approaches towards the guanine moiety, the carbon centre closer to the guanine might experience some electrostatic interactions and its reactivity is expected to change. Earlier observations also suggested that reactivity of a species varies along the IRC [28]. Variations of gas phase (at B3LYP/6-31 + G(d) level of theory) local reactivity parameters of C1 and C2 carbon centres are presented in Figure 4. Local electrophilicity (ω^+) and nucleophilic Fukui function (f^+) is observed to vary sharply around the TS. Importantly, local electrophilicity of C1 centre changes abruptly; however, for C2 centre, variation is not so sharp (Figure 4(a)), which indicates a notable effect on the reactivity of the C1 centre during the alkylation process. Nucleophilic Fukui function of Cl also increases and is observed to vary around the TS. Reverse is observed in case of C2 centre, Figure 4(b). Variation of relative electrophilicity and relative nucleophilicity is depicted in Figures 4(c)–(d). It is interesting to note that, in the ring conformation, relative electrophilicity (s_x^+/s_x^-) of the C1 centre is maximum, and as the reaction progresses, s_x^+/s_x^- values decrease and reach the minimum and again increase (Figure 4(c)). In a usual manner, relative nucleophilicity (s_x^-/s_x^+) exhibits the reverse order. On the other hand, for C2 centre, these two indices exhibit a different trend, not showing any maximum or minimum at the TS; however, importantly a sharp change in the values is observed around the TS (Figure 4(d)). Variation of the local descriptors thus advocates an increase in the electrophilic nature at the C1 centre along the IRC, and this in turn facilitates alkylation. Figures 4(e)–(f) represent variation of gas phase global electrophilicity, chemical potential and global hardness along the IRC. It is seen from the figure that, as '*d*' decreases, chemical potential decreases (more negative) and the system becomes more stable. It is an obvious result because the Az^+ is an electron deficient system, and transfer of electron density towards the species increases its stability. Global electrophilicity exhibits the reverse trend to that of global hardness. We observed similar trends in results at B3LYP/6-311 + + G(d,p) level of theory (Supplementary Material 2).

4.4. Thermochemical analysis

Thermochemical parameters, Gibb's free energy (G), enthalpy (H), activation energy (E_a) and free energy of activation ($\Delta G^\dagger$), were analysed at two different temperatures, 298.15 K (the room temperature) and 310 K (the physiological temperature), using B3LYP/6-31 + G(d) level of theory (Figure 5 and Table 1). We calculated ΔG and ΔH of the adduct formation process, defined as $\Delta G = G_{\text{adduct}} - (G_{\text{aziridinium ion}} + G_{\text{guanine}})$. The observed ΔH values for the process is found to be exothermic with a magnitude of −10.48 kcal/mol at 298.15 K in gas phase and −17.47 kcal/mol in aqueous phase, indicating formation of a more stable adduct in aqueous phase compared to gas phase (Figure 5 and Table 1). However, slight increase in the values is observed at physiological temperature 310 K. Similar trend is observed in case of ΔG values in both phases. Our study thus predicts thermodynamic driving force for adduct formation and is in good agreement with previous observations [15]. Activation energy of the reaction bears more importance, and the gas phase activation energy of the forward reaction (E_{af}) is observed to be 15.88 kcal/mol. However, in aqueous phase, a bit smaller barrier of 15.77 kcal/mol is observed (Figure 5 and Table 1). Earlier, Shukla *et al.* [16] also observed similar energy barrier for mono-adduct formation process. In contrast, the activation energy of the backward reaction (E_{ab}) in gas phase at 298.15 K is found to be 26.68 kcal/mol. This massive energy barrier prevents decomposition of mono-adduct to Az^+ ion and guanine molecule. In aqueous phase this barrier is even higher. This leads to shifting of the equilibrium towards the product side in aqueous phase. The rate constant of the adduct formation is calculated using the thermodynamic formulation of the TST [53,54] at the two temperatures in both phases:

$$k^{\text{TST}} = \frac{k_B T}{h} \exp\left(-\frac{\Delta G^\dagger}{RT}\right), \tag{9}$$

where $\Delta G^\dagger$is the calculated free energy of activation.

Table 1. Thermodynamic parameters involved in alkylation process at B3LYP/6-31 + G(d) level of theory (values in aqueous phase are given in bracket).

	$T = 298.15$ K	$T = 310$ K
ΔH	−10.48 (−17.47) kcal/mol	−10.49 (−17.50) kcal/mol
ΔG	−10.43 (−16.17) kcal/mol	−10.42 (−16.12) kcal/mol
E_{af}	15.88 (15.77) kcal/mol	15.88 (15.77) kcal/mol
E_{ab}	26.68 (33.06) kcal/mol	26.68 (33.06) kcal/mol
$\Delta G^\dagger$	14.38 (14.01) kcal/mol	14.40 (14.02) kcal/mol
k	178.3 (333.0) s^{-1}	450.1 (836.2) s^{-1}

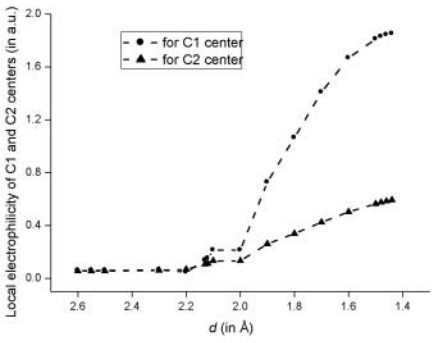

4a: Local electrophilicity of Az^+ ion along IRC

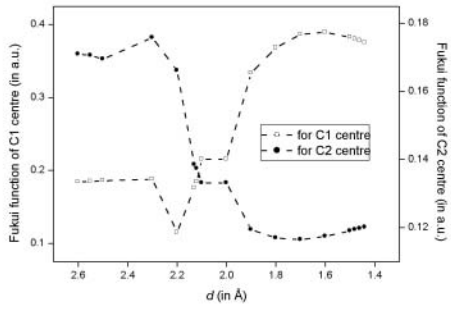

4b: Variation of nucleophilic Fukui function along IRC

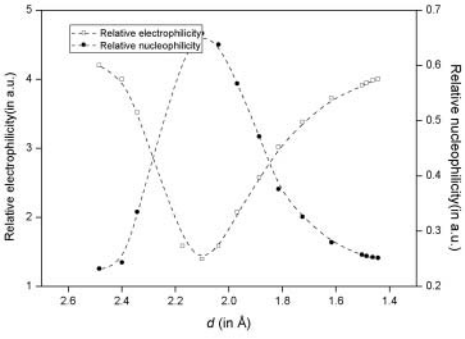

4c: Variation of s_x^+ / s_x^- and s_x^- / s_x^+ at C1of Az^+ ion along IRC

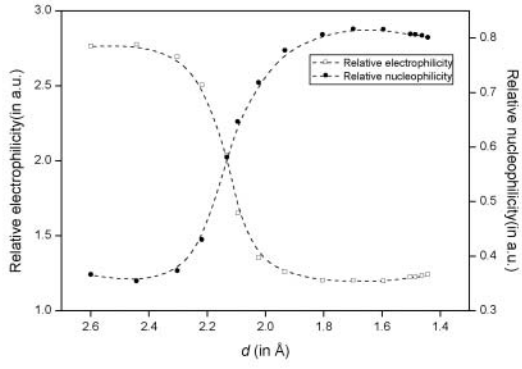

4d: Variation of s_x^+ / s_x^- and s_x^- / s_x^+ at C2 of Az^+ ion along IRC

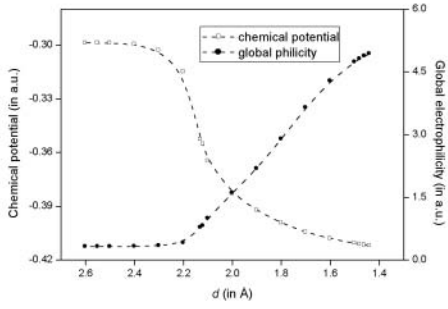

4e. Global electrophilicity and chemical potential of Az^+ ion along IRC

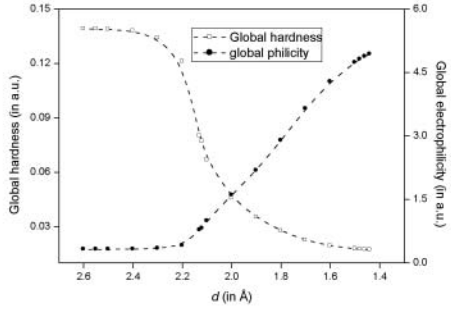

4f. Global electrophilicity and global hardness of Az^+ ion along IRC

Figure 4. Variation of local and global reactivity descriptors.

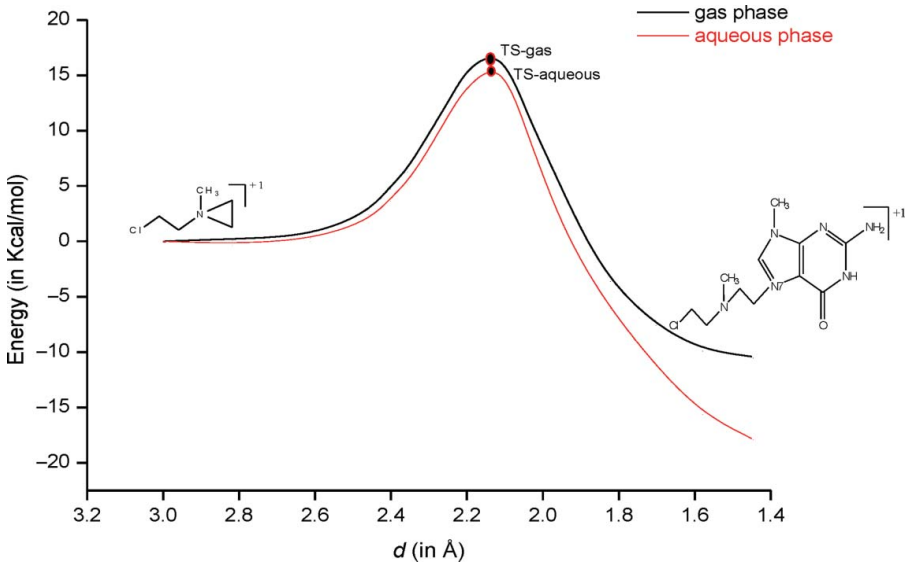

Figure 5. Reaction profile in gas and aqueous phase.

Gas phase $\Delta G^{\dagger}$ for the reaction is 14.38 kcal/mol at 298.15 K and in aqueous phase it becomes 14.01 kcal/mol and we observe little effect of increase in temperature; however, the aqueous phase showed a prominent effect on $\Delta G^{\dagger}$ (Table 1). The gas phase rate constant of the reaction is observed to be 178.3 s^{-1} at 298.15 K that increases to 450.1 s^{-1} at 310 K. We observed a substantial increase in the rate of the reaction in aqueous phase; at 298.15 K, it is 333.0 s^{-1} and 836.2 s^{-1} at 310 K. Thus, we expect an enhanced rate of formation of the mono-adduct at physiological conditions (polar solvent and a temperature of 310 K). Similar trends were observed at B3LYP/6-311 + + G(d,p) level of theory (Supplementary Material 3). High rate of the reaction of Az^+ ion of mustine with guanine moiety agreed with previous observation, which suggests substitution at the N centre of mustine to prepare new analogues [55].

5. Conclusion

Our study reveal that, as the Az^+ ion approaches guanine residue (in DNA), exceptional variation in energy and shape of the LUMO facilitate the alkylation process in spite of the LUMO being associated with the chloroethyl side chain in its typical tricyclic ring geometry. Lowering of LUMO energy also made it easier for the Az^+ ion to head towards forward direction. Further, we observed a sharp variation in local reactivity at the C1 centre of the Az^+ ion (measured in terms of local electrophilicity and nucleophilic Fukui function) around the TS, which act as the facilitating factor for the alkylation process. Thermochemical analysis and rate constant confirmed the thermodynamic driving force for the reaction and an enhanced rate at the physiological conditions.

Earlier studies advocated that alkylation might be facilitated by external electric field or structural variations [56]. However, our present study clearly explains that variation of the local reactivity as well as shape and energy of the LUMO is the driving force for the alkylation process.

Acknowledgements

P.K. Bhattacharyya acknowledges the financial support from Department of Science and Technology (SR/S1/PC-13/2009), New Delhi.

References

[1] S.R. Rajski and R.M. Williams, Chem. Rev. **98**, 2723 (1998).
[2] S. Neidle, in *Molecular Aspects of Anticancer Drug Action*, edited by M. Waring (Verlag Chemie, Weinheim, 1994).
[3] P. Rhoads, J. Am. Med. Assoc. **131**, 656 (1946).
[4] K.W. Kohn, in *Anti-cancer Drugs*, edited by H. Tapiero, J. Robert, and T.J. Lampidis (Colloque INSERM, London, Paris, John Libbley, Euro text, 1989).
[5] A. Gilman and F.S. Philips, Science **103**, 409 (1946).
[6] L.S. Goodman, M.M. Wintrobe, W. Dameshek, M.J. Goodman, A. Gilman, and M.T. Mclennan, J. Am. Med. Assoc. **132**, 126 (1946).
[7] D.M. Noll, T.M. Mason, and P.S. Miller, Chem. Rev. **106**, 277 (2006).
[8] L.F. Provirk and D.E. Shuker, Mutat. Res. **318**, 205 (1994).
[9] S.M. Rink, M.S. Solomon, M.J. Taylor, R.B. Sharanabasava, L.W. McLaughlin, and P.B. Hopkins, J. Am. Chem. Soc. **115**, 2551 (1993).
[10] P. Calabresi, R.E. Parks, A. Gilman, L.S. Goodman, T.W. Raol, and F. Murad, editors, *The Pharmacological Basis of Therapeutics* (Macmillan, New York, 1985).
[11] B. Singer, Nature **264**, 333 (1976).
[12] D.T. Beranek, C.C. Weis, and D.H. Swenson, Carcinogenesis, **1**, 595 (1980).
[13] A. Pullman and B. Pullman, Int. J. Quant. Chem. **18**, 245 (1980).

[14] P.D. Lawley, Prog. Nucl. Acids Res. Mol. Biol. **5**, 89 (1966).
[15] A. Polavarapu, J.A. Stillabower, S.G.W. Stubblefield, W.M. Taylor, and M.H. Baik, J. Org. Chem. **77**, 5914 (2012).
[16] P.K. Shukla, P.C. Misra, and S. Suhai, Chem. Phys. Lett. **449**, 323 (2007).
[17] D.J. Mann, J. Phys. Chem. A **114**, 114 (2010).
[18] J. Hansson, R. Lewensohn, U. Ringborg, and B. Nilsson, Cancer Res. **47**, 2631 (1987).
[19] A. Masta, P.J. Gray, and D.R. Philips, Nucleic Acid Res. **22**, 3880 (1994).
[20] S.M. Rink, M.S. Solomon, M.J. Taylor, S.B. Rajur, L.W. McLaughlin, and P.B. Hopkins, J. Am. Chem. Soc. **115**, 2551 (1993).
[21] M.R. Osborne, D.E.V. Wilman, and P.D. Lawley, Chem. Res. Toxicol. **8**, 316 (1995).
[22] A. Pullman, in *Chemical Carcinogenics, Part A*, edited by J.A.D. Paolo (Marcel Dekker, New York, 1974).
[23] B. Pullman, H. Weinsteins, and J.P. Green, editors, *Quantum Chemistry in Biomolecular Science* (The New York Academy of Science, New York, 1981).
[24] G.B. Bauer and L.F. Provirk, Nucleic Acid Res. **25**, 1211 (1997).
[25] B. Neog, N. Sarmah, R. Kar, and P.K. Bhattacharyya, Comput. Theor. Chem. **976**, 60 (2011).
[26] F.A. Carey and R.J. Sundberg, *Advanced Organic Chemistry Part A: Structure and Mechanism* (Kluwer Academic/Plenum Publishers, New York, 2008).
[27] S. Pal, N. Vaval, and R.K. Roy, J. Phys. Chem. **97**, 4404 (1993).
[28] P.K. Chattaraj, J. Phys. Chem. A **107**, 7068 (2003).
[29] H.B. Schlegel, in *Modern Electronic Structure Theory*, edited by Yarkony (World Scientific Publishing, Singapore, 1994).
[30] R.G. Parr and W. Yang, *Density Functional Theory of Atoms and Molecules* (Oxford University Press, New York, 1989).
[31] J. Melin, F. Aparicio, V. Subramanian, M. Galvan, and P.K. Chattaraj, J. Phys. Chem. A **108**, 2487 (2004) .
[32] J.S.M. Anderson, J. Melin, and P.W. Ayers, J. Chem. Theory Comput. **3**, 375 (2007).
[33] P. Geerlings, F. De Proft, and W. Langenaekar, Chem. Rev. **103**, 1793 (2003).
[34] P.K. Chattaraj, U. Sarkar, and D.R. Roy, Chem. Rev. **106**, 2065 (2006).
[35] R.G. Parr and R.G. Pearson, J. Am. Chem. Soc. **105**, 7512 (1983).
[36] R.G. Parr, R.A. Donnelly, M. Levy, and W.E. Palke, J. Chem. Phys. **68**, 3801 (1978).
[37] T.A. Koopmans, Physica **1**, 104 (1933).
[38] R.G. Parr, L.V. Szentpaly, and S. Liu, J. Am. Chem. Soc. **121**, 1922 (1999).
[39] R.G. Parr and W. Yang, J. Am. Chem. Soc. **106**, 4049 (1984).
[40] F. Mendez and J.L. Gazquez, J. Am. Chem. Soc. **116**, 9298 (1994).
[41] W. Yang and W.J. Mortier, J. Am. Chem. Soc. **108**, 5708 (1986).
[42] R.K. Roy, K. Hirao, S. Krishnamurty, and S. Pal, J. Chem. Phys. **115**, 2901 (2001).
[43] R.K. Roy, S. Pal, and K. Hirao, J. Chem. Phys. **110**, 8236 (1999).
[44] R.K. Roy, S. Krishnamurti, P. Geerlings, and S. Pal, J. Phys. Chem. A **102**, 3746 (1998).
[45] A. Tanwar and S. Pal, J. Chem. Sci. **117**, 497 (2005).
[46] R. Parthasarathi, J. Padmanabhan, M. Elango, V. Subramanian, and P.K. Chattaraj, Chem. Phys. Lett. **394**, 225 (2004).
[47] F.A. Bulat, E. Chamorro, P. Fuentealba, and A. Toro-Labbé, J. Phys. Chem. A **108**, 342 (2004).
[48] M.J. Frisch, G.W. Trucks, H.B. Schlegel, G.E. Scuseria, M.A. Robb, J.R. Cheeseman, G. Scalmani, V. Barone, B. Mennucci, G.A. Petersson, H. Nakatsuji, M. Caricato, X. Li, H.P. Hratchian, A.F. Izmaylov, J. Bloino, G. Zheng, J.L. Sonnenberg, M. Hada, M. Ehara, K. Toyota, R. Fukuda, J. Hasegawa, M. Ishida, T. Nakajima, Y. Honda, O. Kitao, H. Nakai, T. Vreven, Jr. J.A. Montgomery, J.E. Peralta, F. Ogliaro, M. Bearpark, J.J. Heyd, E. Brothers, K.N. Kudin, V.N. Staroverov, R. Kobayashi, J. Normand, K. Raghavachari, A. Rendell, J.C. Burant, S.S. Iyengar, J. Tomasi, M. Cossi, N. Rega, N.J. Millam, M. Klene, J.E. Knox, J.B. Cross, V. Bakken, C. Adamo, J. Jaramillo, R. Gomperts, R.E. Stratmann, O. Yazyev, A.J. Austin, R. Cammi, C. Pomelli, J.W. Ochterski, R.L. Martin, K. Morokuma, V.G. Zakrzewski, G.A. Voth, P. Salvador, J.J. Dannenberg, S. Dapprich, A.D. Daniels, . Farkas, J.B. Foresman, J.V. Ortiz, J. Cioslowski, and D.J. Fox, *Gaussian 09, Revision B.01* (Gaussian, Inc., Wallingford, CT, 2010).
[49] S. Miertus, E. Scrocco, and J. Tomasi, J. Chem. Phys. **55**, 117 (1981).
[50] B. Mennucci and J. Tomasi, J. Chem. Phys. **106**, 5151 (1997).
[51] A. Hamza, H. Broch, and D. Vasilescu, J. Biomol. Struct. Dyn. **13**, 903 (1996).
[52] H. Broch, A. Hamza, and D. Vasilescu, Int. J. Quant. Chem. **60**, **1745** (1996).
[53] H. Eyring, J. Chem. Phys. **3**, 107 (1935).
[54] M.G. Evans and M. Polanyi, Trans. Faraday Soc. **31**, 875 (1935).
[55] R.B. Silverman, *The Organic Chemistry of Drug Design and Drug Action* (Elsevier Academic Press, New Delhi, India, 2012).
[56] P.K. Bhattacharyya and R. Kar, Comput. Theor. Chem. **967**, 5 (2011).